Bioinsp. Biomim. **2** (2007) 42–56 doi:10.1088/1748-3182/2/3/002

A novel distributed swarm control strategy based on coupled signal oscillators

Manfred Hartbauer and Heiner Römer

Department of Zoology, Karl-Franzens University Graz, Austria

E-mail: manfred.hartbauer@uni-graz.at

Received 16 February 2007
Accepted for publication 14 August 2007
Published 10 September 2007
Online at stacks.iop.org/BB/2/42

Abstract

The miniaturization of microrobots is accompanied by limitations of signaling, sensing and agility. Control of a swarm of simple microrobots has to cope with such constraints in a way which still guarantees the accomplishment of a task. A recently proposed communication method, which is based on the coupling of signal oscillators of individual agents [13], may provide a basis for a distributed control of a simulated swarm of simple microrobots (similar to I-Swarm microrobots) engaged in a cleaning scenario. This self-organized communication method was biologically inspired from males of chorusing insects which are known for the rapid synchronization of their acoustic signals in a chorus. Signal oscillator properties were used to generate waves of synchronized signaling (s-waves) among a swarm of agents. In a simulation of a cleaning scenario, agents on the dump initiated concentrically spreading s-waves by shortening their intrinsic signal period. Dirt-carrying agents localized the dump by heading against the wave front. After optimization of certain control parameters the properties of this distributed control strategy were investigated in different variants of a cleaning scenario. These include a second dump, obstacles, different agent densities, agent drop-out and a second signal oscillator.

1. Introduction

Microrobot swarms provide the possibility of enhanced task performance, higher reliability and lower unit complexity when compared with traditional robotic systems. Swarm coordination in a large group of robots is a challenging problem requiring an elaborate control and communication strategy [11, 22, 26]. However, there is a tradeoff between robot miniaturization and energy supply, agility, signaling and perception capabilities. Consequently, swarm control needs to be adapted to limitations in these parameters. Robot swarm coordination frequently makes use of the following technical solutions: a central processor [22], an elaborate collision avoidance system, map knowledge for detailed motion planning [28, 38], self-positioning systems, distance measurements among swarm members and landmark localization [30]. Most of these techniques require an elaborate communication strategy between agents, and between agents and beacons or a central processor.

Currently, microrobots only a few millimetres in size acting in a large swarm should be able to accomplish a cleaning task without making use of these communication solutions. The present study describes a biologically inspired distributed swarm control strategy for a swarm of primitive microrobots that accomplishes a complex cleaning task relying on self-organization.

Cooperation among robots arises in a self-organized manner when robots move towards the highest concentration of crumbs which were dropped by others [34]. This nature-inspired navigation is ant-like and was implemented in the foraging strategy of a group of robots [10, 27]. Gradient sensing and an extended sensor range is one of the prerequisites for the successful application of this swarm strategy. Microrobots exhibit a very limited sensor range and gradients will therefore be hard to detect due to their small dimension. Different to the initial condition of chip sorting scenarios [6, 37] in which chips are more or less clustered in the arena, only two dirt piles were simulated in the cleaning

scenario of the current study. Simulated agents do not have a global knowledge about the position of other agents or about the position of dirt piles or the dump and transfer the grains of dirt following a simple rule-set.

The characteristics of the simulated agents are very similar to those of the I-Swarm microrobots, which are currently under construction and represent the key goal of the current EU-project 'I-Swarm'. These small microrobots (2×2 mm) communicate via faint light flashes with a very limited signal range with sensing restricted to four primitive photocells, which does not allow the accurate estimation of signal direction. Neither signaling nor perception is omni-directional and regular blind spots are evident. There is no hardware enabling collision avoidance.

Hartbauer and Roemer [13] suggested an oscillator-based biologically inspired communication strategy which, applied to a swarm of stationary microrobots, resulted in the self-emergent generation of waves of synchronized signaling (s-waves). Together with a rule-based reaction the coupling of signal oscillators of individual agents should enable the successful accomplishment of various scenarios of a cleaning task despite limitations mentioned above. Thus far, coupled oscillators have been used in robot design for the integration and transfer of multi-sensor inputs into a motor drive signal in a time-varying environment by using a relatively simple algorithm [5, 36]. Nonlinear oscillators have also been used for the control of group size near a beacon in a medium-sized group of robots [15]. Further coupled oscillators were used to control the morphology of a modular robot [17] and for the reformation of a group of robots equipped with a rotating laser-scanning distance sensor [20]. To guide dirt-carrying agents in the current simulation study to a dump, agents head against the wave front of s-waves, which spontaneously emerge if agents synchronize their signal oscillators with a primitive flash signal. In a simulation with stationary agents the synchronization of signal oscillators was found to be very robust to signal masking, resilience, communication obstacles, signal intensity fluctuations and cycle length fluctuations [13]. Robustness of oscillator synchronization to fluctuations of coupling strength and to variability of intrinsic signal periods was also found in the Kuramoto model of coupled oscillators [18].

The idea for such signaling waves was derived from male bushcrickets (*Mecopoda elongata* (*M. elongata*)), which acoustically synchronize their sound signals by coupling their song oscillators with other males [12]. Since synchronization in a bushcricket chorus is not perfect, the result is a leader–follower relationship between signals with one leading the other by some tens of milliseconds. In a choice situation females were found to prefer leaders [29], and leaders in a chorus are those who exhibit a faster song oscillator during solo singing [12]. Orientation towards the leader in a chorus is an elegant way to cope with a high degree of signal jamming and allows females to choose among males in an aggregation. In the cleaning scenario agents carrying grains of dirt use a similar tactic by heading towards the next local leader (agents which signal first). This reliably guides them to the location where s-waves are initiated, the dump.

The cleaning scenario used in the current work shows some similarities with the foraging scenario described for multi-agent robotic teams [1, 9, 24]. Nevertheless the swarm control strategy which was used to accomplish the search and retrieval task is different form the oscillator-based approach. In the study of Balch and Arkin [1] a team of eight medium-sized robots foraging attractive objects could improve their performance by simple state communication, allowing other robots to sense the current state of a robot. The currently proposed swarm control allows agents in a swarm to communicate the direction of a target in an indirect way by initiating s-waves spreading out in concentric waves from agent to agent. The establishment of signaling waves propagating through the arena is a by-product of oscillator coupling in a swarm of agents exhibiting a limited sensor range. This self-emerging property of signal oscillator coupling was used as a navigation cue directing agents to an attractor (e.g. dump). This strategy is similar to the wave-front path planning algorithm and was already successfully implemented in the navigation of robots in a dynamic environment in which obstacles appeared and disappeared [25]. In the study of O'Hara and Balch robots were guided by a grid of stationary signal relays (nodes) computing a distributed Bellman–Ford algorithm [3]. In contrast, agents in the current study function as mobile nodes taking part in the propagation of s-waves. This approach is fundamentally different to signal transfer used in a group of robots covering arena space in an optimized way [16] or a hop-count transmitted from agent to agent [14]. Therefore, the suggested oscillator-based approach used to navigate a swarm of primitive agents in a cleaning scenario represents a novel strategy of swarm control.

In the current simulation study certain swarm control parameters were optimized and the navigation strategy was investigated for its robustness to agent drop-out, signal intensity fluctuations and signaling obstacles. Further inherent properties of the oscillator-based control strategy were elucidated in different variants of a cleaning scenario. This includes competition between two dumps and collective decision. Finally, a second signal oscillator was implemented which guides agents in search of a dirt pile to this location. This simulation study allows some predictions concerning the performance of a swarm of real I-Swarm robots in similar scenarios and provide the basis for a proper design of rule-based microrobot behavior.

2. Methods

2.1. I-Swarm microrobot properties

The properties of simulated agents used in the current study are based on hardware and software features that will be realized in the I-Swarm microrobot. I-Swarm microrobots will have a size of about 2 mm and a quadratic shape. A constant light source powers two miniature solar cells mounted at the top of each robot, limiting agent activity to the brightly lit robot arena. Locomotion is based on three to four piezo-electrically driven legs, allowing a maximum speed of 10 mm s^{-1}, although due to energy consumption a much slower speed may be expected

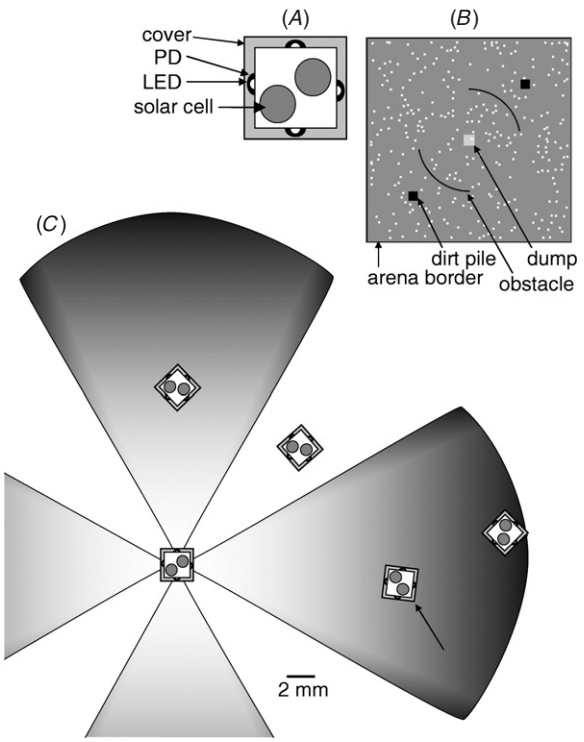

Figure 1. The appearance of the I-Swarm microrobot, the standard cleaning scenario and the geometry of the communication system. A bird's-eye view of an I-Swarm microrobot is given in (*A*). Two solar cells on top of the robot maintain energy supply provided by a constant light source. Under a cover (gray area) there are four photodiodes (PDs) and four light emitting diodes (LEDs) facing different directions. The standard cleaning scenario consists of two dirt piles (black squares) and a central dump (gray square) as shown in (*B*). Two large obstacles can be implemented in a cleaning scenario. Agents are shown as white dots. A schematic illustration of the signaling geometry of simulated agents is given in (*C*). In the given arrangement a supra-threshold signal is only detected by one (arrow) of four neighbors in the proximity of a signaling agent.

($\sim$0.1 mm s^{-1}). Robots are unable to perform turns without simultaneous forward or backward locomotion. Angular turns are limited to 2° per step and microrobots will be able to move backwards. Since forward speed as well as backward speed is currently unknown, simulations of cleaning scenarios with different agent locomotion speeds were performed.

Communication among I-Swarm robots is based on flash light signals, which are simultaneously broadcast from four light emitting diodes (LEDs) and received by four photodiodes (PDs). Each of these hardware components is facing in four different directions (figure 1(*A*)). Between neighboring LEDs and PDs there is a 30° blind spot. The direction of detected signals can only be assigned to one of the four photodiodes without any further directionality. Microrobots are not equipped with any active collision avoidance system. After collisions, agents free themselves by continuing to turn as long as forward (or backward) locomotion is blocked. An indirect proximity warning of the arena border may come from the light, which powers the pair of solar cells. After entering a dim region, robots 'know' that they entered the border zone of the arena.

Since I-Swarm microrobots are not able to pick up objects and drop them somewhere, the transport of particles by real I-Swarm microrobots will be limited to the simulation of carrying particles. In the simulation this was achieved by switching an internal state variable '*carry*'. But by altering the light powering solar cells at certain spots (e.g. a different light intensity, or by switching to another wavelength) the location of a dump area and a dirt pile can be realized. Therefore, in the currently proposed cleaning scenario the number of available dirt particles is kept at a constant size throughout a simulation run.

2.1.1. General model description. A swarm simulation was developed in order to study the emergent behavior of many hundreds of identical I-Swarm microrobots after the implementation of the oscillator-based control strategy. This simulation was developed in Netlogo 3.0.2 (http://ccl.northwestern.edu/netlogo/), a widely used multi-agent simulation environment.

At the beginning of each simulation run an initialization procedure was completed resulting in a random distribution of a homogeneous population of agents in the simulated arena. Subsequently, agents were forced to move in a random walk until a minimum distance of four patches to any neighbors was achieved. Depending on the number of agents, this resulted in a spacing with high and low density areas at the beginning of a simulation run. Simulated agents were equipped with a signal oscillator which triggers a faint light flash in the last oscillator tick (if *cycle-counter* = *cycle-length*). Agents in close proximity used this signal to synchronize their signal oscillators. Due to the limited signal radius only a small amount of neighboring agents signal in synchrony. After a few oscillator cycles waves of synchronized signaling (s-waves) spread out through the arena. These waves were initiated at the dump area and were used as guidance cues by dirt carrying agents in a cleaning scenario. The standard cleaning scenario (SCS) consisted of two dirt piles and a centrally positioned dump (figure 1(*B*)). Unless stated differently 250 agents were simulated in this scenario moving at a speed of 0.2 patches per step. The swarm simulation allowed the implementation of two large obstacles in the cleaning scenario.

First, the model parameters shown in table 1 were optimized in the SCS. In a second step an optimized parameter set was used to establish different cleaning scenarios which allowed the investigation of collective decision making and the implementation of a second signal oscillator, which guides agents in search of dirt to the dirt piles. All runs were performed using the oscillator and communication parameters shown in table 2. The simulation was restricted to two dimensions corresponding to the properties of a flat arena.

Model parameter optimization. Delivering as much dirt particles in a certain time period was the goal of the parameter optimization procedure. A two-step approach was chosen in order to optimize those parameters (listed in table 1) possibly affecting the performance of the swarm control strategy in the SCS. First, a suboptimal parameter set was found by interactive parameter control. In a second step a fine-tuning of each

Table 1. Simulation parameters optimized in the standard cleaning scenario.

Parameter	Unit	Range	Optimization step length	Optimum
Number of agents	(*N*)	250–350	50	300
Agent speed	(Patches per step)	0.20–0.45	0.05	0.35
Maximum number of cycles to wait at the dump area = *cycles-wait*	(*N*)	5–20	5	15
Leader window size	(steps)	3–10	2, 3	8–10

Table 2. Oscillator and signaling parameters.

Parameter	Units	Value (range)
Intrinsic signal period	(steps)	30 ± 1
Intrinsic SP of agents at the dump	(steps)	25 ± 1
Slope of the branches representing the PRC	(arbitrary units)	0.8
Transition phase	(arbitrary units)	0.5
Maximum signal radius	(patches)	20
Signal intensity	(arbitrary units)	100 ± 0.5
Detection threshold	(arbitrary units)	30

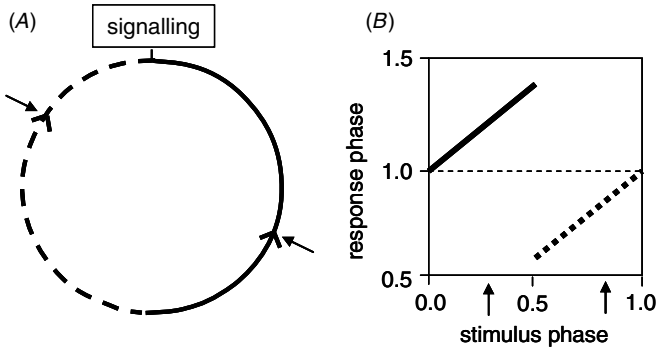

Figure 2. The properties of the signal oscillator. The oscillator cycle of signal oscillators can be regarded as a circle (*A*) which is incremented in each simulation step by one clock tick. In the last tick of the oscillator cycle, a signal is emitted. Upon detection of a supra-threshold signal in the first half of the cycle (right arrow in (*A*) and left arrow in (*B*)) the length of the disturbed cycle is increased. The oscillator clock moves backwards resulting in a prolongation of the oscillator cycle. After the perception of a supra-threshold signal late in the oscillator cycle (left arrow in (*A*) and right arrow in (*B*)) the cycle is shortened and the oscillator clock moves forward. This oscillator behavior is determined by the properties of the underlying phase response curve shown in (*B*).

parameter was achieved by performing repeated simulation runs investigating a certain value range of a single parameter while holding all other parameters at a constant value (see table 1). Each individual parameter combination was investigated in at least 10 simulation runs for its influence on the total number of delivered dirt particles after a minimum simulation period of more than 5000 simulation steps.

2.1.2. Signal oscillator properties. Details concerning oscillator properties of the synchronizing bushcricket species *M. elongata* can be found in [12] and [33]. Oscillator properties that resulted in a quick and robust establishment of synchronization waves (s-waves) in a swarm of stationary microrobots have been described elsewhere [13] and were fully implemented in the current simulation (see table 2). Oscillator coupling of neighboring agents leads to a local synchronization of signaling activity and results in the self-emergent generation of s-waves. Oscillator coupling was realized as follows: at the beginning of each simulation run, every agent starts its signal oscillator at a random phase. In each simulation step the signal oscillator clock is incremented by one and is reset to zero after completion of the cycle. Each agent emits a faint light flash in the last tick of its signal oscillator cycle (figure 2(*A*)). After the perception of a suprathreshold signal (a flash emitted by neighbors) the disturbed cycle length is either prolonged or shortened (arrows in figure 2). The resulting change in length of the disturbed cycle depends on the stimulation phase and was calculated after equation (1):

$$phase\_of\_perturbation = \frac{cycle\_counter}{cycle\_length}. \quad (1)$$

The change of oscillator phase (*phi*) following a perturbation was calculated after the phase response curve (PRC) (figure 2(*B*)) characterizing the song oscillator properties of *M. elongata* males. The shape of the PRC (figure 2) used in the current simulation was optimized in a scenario with stationary robots in order to establish s-waves as quick as possible [13] (see figure 3). Oscillator behavior was modeled on the basis of two linear equations representing individual branches of the PRC (the slope of both branches: 0.8). A perturbation in the phase smaller than 0.5 resulted in a cycle prolongation calculated after equation (2). In contrast, a perturbation in the phase above 0.5 resulted in a shortening of the disturbed cycle length and was calculated after equation (3). Only the phase of a supra-threshold stimulus, but not stimulus intensity itself, affects the change in length of the disturbed cycle. Signal oscillators could be perturbed several times in a single oscillator cycle.

$$phi = 1 + (0.8 * phase\_of\_perturbation) \quad (2)$$

$$phi = 1 + (0.8 * (phase\_of\_perturbation - 1)). \quad (3)$$

The perturbed oscillator phase shows some Gaussian distributed randomness with a standard deviation of 0.009. The length of the disturbed cycle was calculated after equation (4):

$$new\_cycle\_length = cycle\_length * (phi \pm 0.009). \quad (4)$$

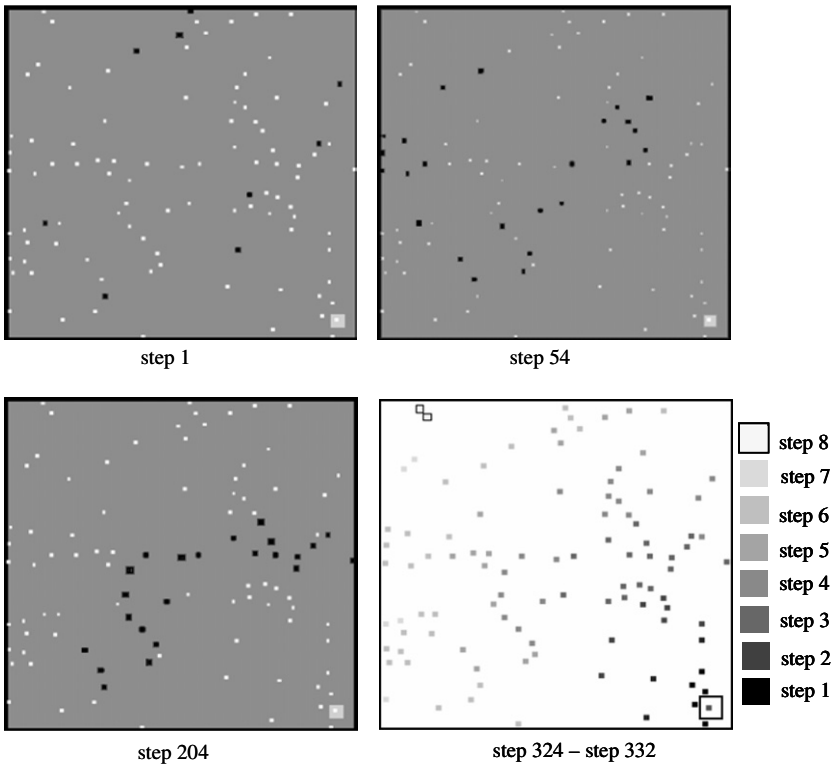

Figure 3. Establishment of synchronization waves (s-waves). In a simulation which allows us to study the establishment of s-waves immobile agents (dots) were randomly distributed in the arena at the beginning. Agents started at a random phase in their oscillator cycle and signal in the very last phase of their cycle (agents drawn in black). One agent exhibits a slightly faster oscillator cycle and is located at the lower right corner of the arena. After 50 simulation steps this agent triggers waves of synchronized signaling (s-waves) which spread out through the arena within only 8 simulation steps. These waves are generated in every oscillator cycle and were used as a guidance cue in the cleaning scenario.

The remaining cycle length was calculated according to equation (5):

$$cycle\_counter = \text{round}(new\_cycle\_length - cycle\_counter). \tag{5}$$

Fluctuations in the free-run period of oscillators (intrinsic SP, '*cycle_length*' = 30 steps) as well as cycle-to-cycle variations in the cycle length of oscillators exhibited a standard deviation of 1 simulation step. This simulates the variability of the timers of the I-Swarm microrobots, which are of limited precision.

2.1.3. Swarm control strategy. S-waves were triggered at the dump by agents exhibiting a shorter intrinsic SP (25 steps). After a few oscillator cycles s-waves spread throughout the arena allowing dirt-carrying agents to locate the dump. They do so by heading towards the first signaler among their neighbors that is detected in the last part of their oscillator cycle ('*leader-window*'). If a signal in the '*leader-window*' is missed then dirt-carrying agents maintain the current heading. In the SCS only agents located at the dump trigger s-waves whereas in the 'two-oscillator scenario' agents at the dirt pile trigger s-waves too. This was realized by the synchronization of the second oscillator among local agents.

In long lasting simulation runs simulating a larger swarm (>300 agents) the delivery of dirt particles gradually decreased because of a jam of newly arriving dirt-carrying agents at the dump. This unwanted mass effect could be successfully abolished by use of a dynamic '*cycles-wait*' variable instead of a fixed one. This was achieved by a simple behavioral rule: agents waiting at the dump stop waiting with a probability of 50% as soon as they simultaneously perceive two signals of high intensity on two different PDs, which is thought to be associated with an overcrowded dump. In all simulations the maximal '*cycles-wait*' was restricted to 15 cycles and agents are moving away from the dump by performing a pseudo-random walk neglecting the dump area for the next 900 time steps.

A detailed instruction scheme which every agent executes in each simulation step was summarized in figure 4. The first three instruction blocks decrement count-down variables and increment the cycle clock by one. Agents broadcast a faint signal in the last tick of their signal oscillator which is perceived by neighboring agents as long as they are in the range of the signal and no other agents block signal transmission between a sending and a receiving agent (instruction block 5). If agents perceive a signal, their oscillator phase will be perturbed (instruction block 6) and the maximum signal intensity is stored for the performance of active collision avoidance behavior or for the dynamic regulation of agent density at the dump. Agents carrying dirt particles or in search of dirt particles move according to their behavior state

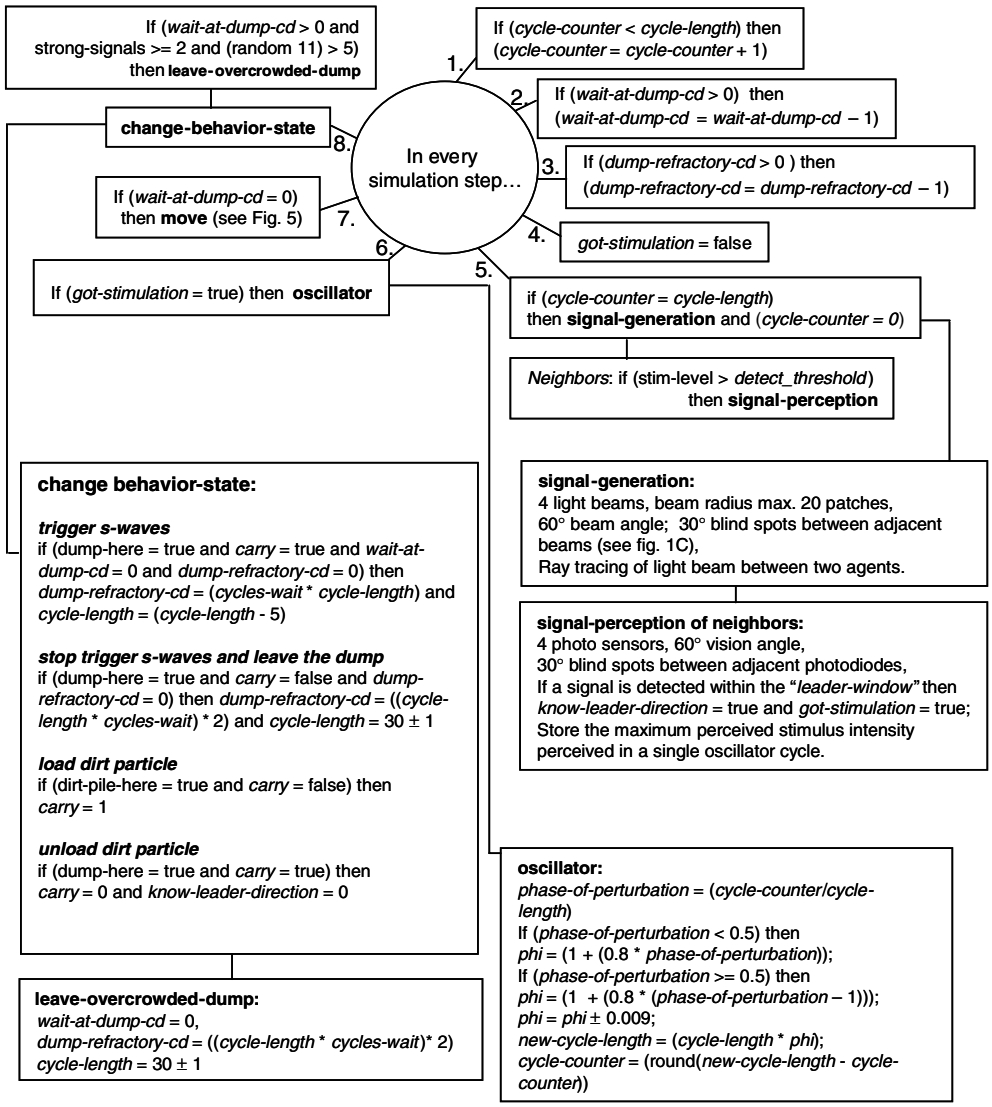

Figure 4. Instruction blocks executed by every agent in each simulation step. All agents execute eight logical program blocks in each simulation step. Agents could not execute the next block before all other agents finished the current block. ∗-cd refers to a variable holding a value that is count down by 1 in every simulation step.

(see scheme illustrated in figure 5). Instruction block eight in figure 4 enables agents to properly change their behavior state.

2.1.4. Simulated microrobot arena. The simulated robot arena (figure 1(*B*)) consisted of a square of 100 × 100 patches containing many hundreds of agents each having a size of 2 × 2 patches. Two dirt piles (clusters of dirt particles) were given fixed positions on the diagonal axis from the upper right corner to the lower left corner. Each dirt pile was represented by a square of 9 × 9 patches. The dump was represented by a square consisting of 10 × 10 patches and was positioned either in the middle of the arena for the SCS or near the lower right corner. In simulations with a second dump, one dump was positioned near the lower right corner and an additional dump (of the same size) was positioned near the upper left corner.

2.1.5. Signaling and perception properties of simulated agents. The signaling and perception properties of agents in the swarm simulation were derived from the hardware specifications of the I-Swarm microrobot. Communication between agents is based on faint flash signals (one stimulation step in duration) from four light emitting diodes (LEDs) facing four different directions. The signaling geometry is illustrated in (figure 1(*C*)). All four LEDs simultaneously emit a light flash creating a 60° cone in which the signal intensity was fixed to 100 in a radius of 10 patches and decreases over distance according to an inverse square law at a greater distance equation (6). The maximum light intensity showed some variation between individual agents. The variation was taken from a Gaussian distribution with a mean of 100 (arbitrary units) and a standard deviation of 0.5. Together with a detection threshold (fixed to 30) these parameters resulted in an average maximum signal radius of 20 patches:

$$level = \frac{100}{\left(\frac{distance}{10}\right)^2}. \tag{6}$$

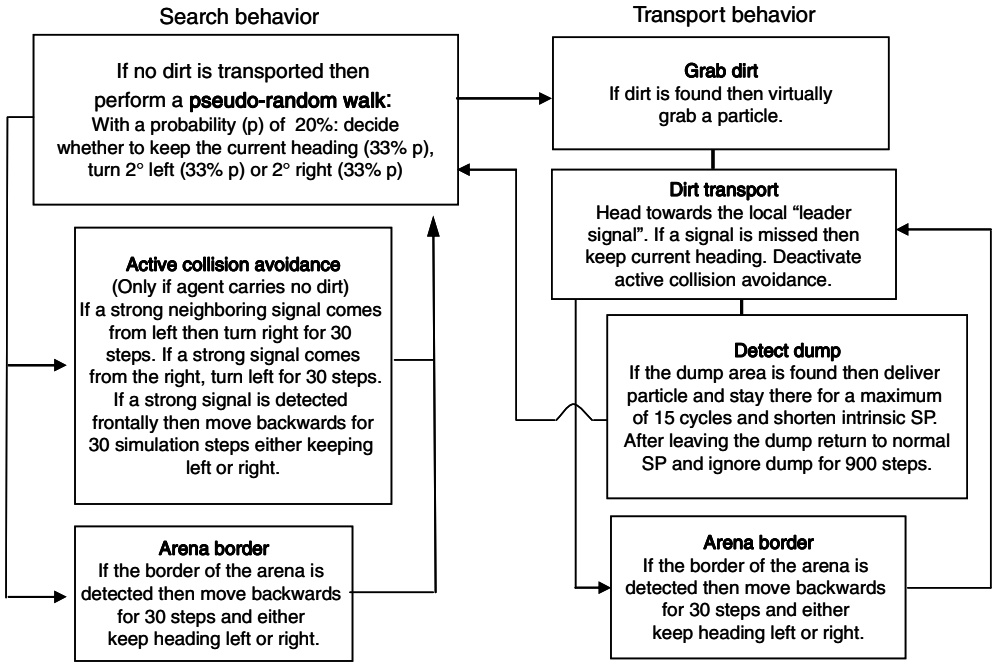

Figure 5. Behavior scheme. In the cleaning scenario the simulated behavior of individual agents is divided into two distinct behavior sets: the search behavior, and after encountering a dirt particle, the transport behavior. The major differences between the two behavior sets are that searching agents perform a pseudo-random walk and dirt-carrying agents do not perform active collision avoidance while heading against the wave front of s-waves.

Additionally, signal intensity decreases laterally off the center axis (angle) by a maximum of 60%. This lateral decrease of light level was modeled according to equations (7) and (8) in order to simulate the intensity profiles of real LEDs:

$$perc\_intensity = (-0.0089 * angle^2) - (0.559 * angle) + 105.88 \quad (7)$$

$$level = \frac{(level * perc\_intensity)}{100}. \quad (8)$$

Signaling cones of two neighboring LEDs form a blind spot of approximately 30°. Perception of light signals was realized by four PDs facing in the same direction as the four LEDs. They also share the same geometry concerning blind spots as caused by the arrangement of LEDs. A supra-threshold signal will only be received when the spatial arrangement of two agents allows a direct signal path from the signaling LED of the sender to one PD of the receiver (figure 1(*C*), arrow pointing to such a receiver). At the receiver side the direction of a leader signal can only be assigned to one of the four PDs, thus stimulus direction can only be roughly estimated (precision = ∼90°). Because of this fact a randomization of the movement of dirt-carrying agents was not implemented in the simulation.

2.1.6. Motion control. The movement of each agent in a swarm is defined by distinct behavioral rules, which were adapted to two principally different tasks: search and transport. At no time do agents have global knowledge of the simulation. A behavior network (similar to [23]) was used which results in complex behaviors, which emerge through the interaction of simple behavior rules (illustrated in figure 5).

2.1.7. Search behavior. Agents are blind to dirt particles and to the dump, and only detect them after accidental encounters. In a swarm of agents performing a random walk, dirt piles and the dump are quickly detected. Since agent locomotion is restricted to turn angles of 2° per step, a movement strategy was defined which results in a pseudo-random walk. This was found in a walk in which every agent decides to change the current heading at each simulation step based on the following probabilities: individual agents keep their current heading with a probability of 80%. In the remaining 20% of cases they keep the current heading with a probability of 33.3% or either turn 2° either left or right with a probability of 33.3% each. This kind of random walk prevented agents from circling and decreases the probability of large gaps lacking agents.

2.1.8. Active collision avoidance. In the swam simulation flash signals emitted by agents may be used not only for the synchronization of signal oscillators but may also be used in active collision avoidance. The following strategy was investigated with regard to its influence on the performance of the swarm in the SCS: an intense flash signal (>99 arbitrary units) perceived by the frontal LED of any agent indicated a very close agent ahead. This resulted in a backward movement for the duration of 30 steps heading towards a randomly chosen direction. An intense signal perceived by one of the lateral LEDs started an evasive behavior towards the opposite side for the next 30 simulation steps. If another intense flash is perceived during an avoidance behavior, a new avoidance behavior will be initiated immediately. It turned out that in order to reach the dump in a reasonable amount of time, dirt-carrying agents need to switch off their agent avoidance

behavior and rely on the collision avoidance of others. This resulted in a much faster delivery of particles to the dump area. Due to the blind spots of the signaler and the receiver, this type of active collision avoidance only worked properly if the spatial arrangement allowed the detection of a signal by one of the four PDs of the receiver (figure 1(*A*)).

If an agent detected the border of the arena after entering a dim region, it moved backwards for 30 cycles and kept heading either left or right with a probability of 50%. This motion rule let agents move away from the arena borders creating a bended motion trajectory. If a second collision occurred during this maneuver, agents started to move forward again.

2.1.9. Collisions. In the case of a collision occurring between agents or between an agent and an obstacle, either a passive or active escape strategy is possible: the passive strategy relies on the possibility that agents involved in a collision are still capable of rotating as long as forward locomotion is blocked. Here individual agents do not even recognize a collision. A negative side-effect of this strategy is the amount of time agents spend in escaping from collisions. Therefore, the total amount of simulation steps agents spent in escaping from collisions was added up in a collision-counter. The active escape strategy was based on collision sensors (one on the front side and one on the rear side). A backward motion is initiated after a collision is detected by the front sensor. This backward motion is maintained for 30 steps either turning towards the left or the right side. If an additional collision is detected by the sensor on the rear side, agents start to move forward again.

2.1.10. Motion hierarchy. In all cases in which the forward or backward locomotion is blocked by an obstacle or by another agent, agents are only capable of turning. As soon as the agent moves backward (e.g. after detecting the border of the arena), all other behavior rules will be suppressed for the next 30 steps. Active collision avoidance lets agents stop their search for dirt particles for the duration of their avoidance behavior (30 steps). Agents only performed a pseudo-random walk when they were not moving backward, or if they were not engaged in active collision avoidance maneuver.

2.2. Performance metrics

Depending on the metrics used for the quantification of swarm performance in multiagent robot systems there is a tradeoff between the goal of the scenario and the costs associated with the accomplishment of that goal [1]. The main goal of the cleaning scenario is the delivery of a maximum quantity of dirt particles within a certain amount of simulation steps. The costs associated with the accomplishment of this goal were represented in the path lengths of dirt-carrying agents and in the time spent in escaping from collisions. Since the number of available dirt particles is constant throughout a simulation run, swarm performance was quantified by the number of delivered dirt particles at the dump within 5000 simulation (10 000 steps in scenarios with two oscillators).

In order to compare the costs with the quantity of delivered dirt particles between different scenarios a path index was calculated. This index was calculated by dividing the average path length of dirt-carrying agents by the number of delivered dirt particles. A low path index indicated a high swarm performance.

The tradeoff between the time (steps) each agent spent in escaping from collisions and the quantity of delivered dirt particles was investigated by the calculation of a collision index. This index was calculated by dividing the average number of simulation steps each agent spent in escaping from collisions by the number of delivered dirt particles. A low collision index indicates that agents spent only a short time in collisions compared to the number of delivered particles.

2.3. Two-oscillator simulation

Swarm control in a cleaning scenario may be improved by the implementation of a second signal oscillator in each agent. The intrinsic SP of oscillator I is shortened at the dump and triggers s-waves guiding dirt-carrying agents to the dump (the same as in the SCS). The intrinsic SP of oscillator II is shortened at the dirt pile and triggers a second set of s-waves guiding agents in search of dirt particles to this location. The implementation of a second oscillator made it necessary that agents emit two different kinds of signals. In a real robot scenario this could be realized by a flash and a double flash, both lasting for one simulation step. In simulations of a second oscillator, care was taken that only one kind of signal was emitted within a single simulation step. Additionally, active collision avoidance was deactivated for agents searching for dirt particles that perceived a 'leader signal' in the final phase of the oscillator cycle of oscillator II.

In such a scenario almost all agents searched for a dirt particle at the beginning of a simulation run. This, however, resulted in an aggregation of almost all agents at the dirt pile and interrupted the propagation of s-waves from agent to agent. For the maintenance of s-wave propagation it was therefore necessary to prevent a certain percentage of agents from heading against any wave-front. These agents function as relays (20% of all agents). In order to prevent a jam of agents at the dirt pile the maximal '*cycles-wait*' of agents there was limited to five oscillator cycles.

2.4. Statistics

Sigma Stat 3.0 (Statsoft Inc.) was used for all statistical analysis. The difference between the means of two groups was tested for its significance by an unpaired *t*-test for data exhibiting a normal distribution. If a normal distribution was absent, a Mann–Whitney *U* test was performed. When the difference between the means of more than two groups was tested for its significance a one-way ANOVA followed by a Tukey's post hoc test was performed. If the data did not follow a normal distribution, a one-way ANOVA on ranks was performed followed by a Dun's post hoc test.

3. Results

Simulation results are structured in three major parts: first, the results of simulation runs are shown that investigate the

influence of a certain parameter range or a certain variant of swarm strategy in the SCS (3.1). Second, the results of simulation runs are presented that investigate the robustness of the swarm control strategy in the SCS (3.2). Finally, the suggested swarm control strategy was implemented in alternative variants of the cleaning swarm scenario (3.3).

3.1. Establishment of s-waves in a swarm of mobile agents

At the beginning of each simulation run, the oscillators of individual agents started at a random phase in their oscillator cycle. After about 200 simulation steps (about seven oscillator cycles), waves of synchronized signaling (s-waves) started to propagate throughout the robot arena. Despite spatial limitations of both signaling and perception and a constant change of local agent density, concentric s-waves quickly spread out from agent to agent in a self-organized manner. At an early stage of s-wave establishment, two s-waves often interfered and canceled each other out at regions of interference. In the following oscillator cycles, one s-wave finally replaced others. The faster oscillator speed of agents at the dump resulted in the initiation of s-waves which successively replaced an already established s-wave. As long as the dump was occupied, spiral waves were completely absent and s-waves started to spread out in concentric waves. After an abrupt change of the location of the dump, s-waves spread out from the new dump location as soon as agents localized the dump. In simulation runs differing in the swarm size (250, 300 and 350 agents), s-waves spread out at a similar average speed of 9.7 patches per step ($p > 0.05$, one-way ANOVA, 12 simulation runs for each group).

3.1.1. Influence of active collision avoidance. In the swarm simulations, active collision avoidance was initiated after detecting a signal of high intensity indicating a close neighbor. In simulation runs with active collision avoidance, the percentage of simulation steps that each agent spent in escaping from collisions was significantly lower ($11.6 \pm 0.5\%$, $p < 0.001$, Mann–Whitney U test, $n = 12$) compared to those simulation runs without active collision avoidance ($21.3 \pm 2.6\%$). Furthermore, the implementation of active collision avoidance led to a significant improvement ($p < 0.001$, Mann–Whitney U test, $n = 12$) of the performance of the swarm in the standard cleaning scenario (SCS). This was obvious by a significantly higher quantity of dirt particles delivered after 5000 simulation steps (44.6 ± 4.1 with collision avoidance versus 30.9 ± 7.2 without collision avoidance, $p < 0.001$, Mann–Whitney U test, 12 simulation runs for each group). All further simulations were therefore performed using active collision avoidance.

3.1.2. Escape strategies. Compared to the active escape strategy the passive escape strategy did not require collision sensors and resulted in a significantly better swarm performance. This was obvious from a significantly smaller average number of delivered dirt particles at the end of the SCS simulating an active escape strategy (28.2 ± 4.7 particles versus 46.0 ± 4.2 particles, $p < 0.001$, t-test, 12 simulation runs for each group). In simulations using the active escape strategy about half of all agents were constantly performing a backward movement, thereby decreasing swarm performance. Because of these results, the passive escape strategy was used to free agents engaged in collisions in all further simulations.

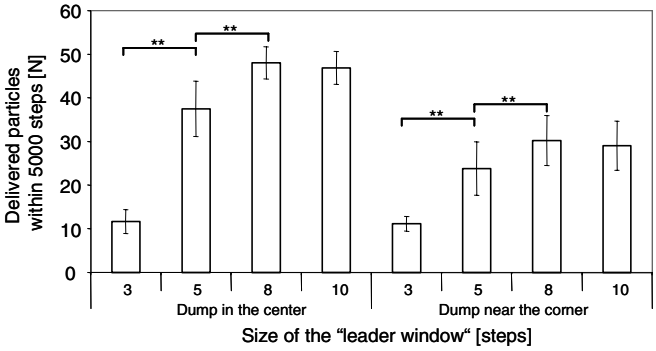

Figure 6. Influence of the size of the 'leader window' on swarm performance. The influence of the size of the 'leader window' was investigated in the standard cleaning scenario (shown in figure 1(*B*) without obstacles) and after positioning the dump near the lower right corner of the arena. Swarm performance, which was quantified by the number of delivered particles, increased as a result of widening the 'leader window'. At 10 time steps no further improve of swarm performance was observed. ** indicates a $p < 0.001$.

3.1.3. Optimization of the 'leader window'. Dirt-carrying agents were guided to the dump by heading towards the first signal in a certain time window ('*leader-window*') at the end of their own oscillator cycle. The influence of this parameter on swarm performance was investigated in the SCS. The mean quantity of dirt particles delivered within 5000 steps significantly increased with the size of the 'leader-window' up to a window duration of 8 simulation steps ($p < 0.001$, one way ANOVA followed by a Tukey's Post Hoc test, 12 simulation runs for each group, see figure 6 (left block)). In a modified version of the SCS dirt carrying agents had to locate a dump area positioned near the lower right corner. This resulted in a doubling of the shortest path that each dirt-carrying agent had to master in order to reach the dump. Again a '*leader window*' of 8 or 10 steps resulted in the best swarm performance in this modified SCS (figure 6 (right block)).

3.1.4. Influence of agent density and speed. Simulations performed at different agent densities and locomotion speeds showed a strong influence of speed but only little influence of swarm size on the number of delivered particles (figure 7(*A*)). With increasing swarm performance at longer step lengths the average percentage of simulation steps that each agent spent in escaping from collisions increased too (figure 7(*B*)).

The highest number of delivered particles (about 130) was obtained in simulation runs simulating 300 agents moving at a step length of 0.4 or 0.45 patches. However, in long lasting simulation runs (15 000 steps) simulating larger swarms (300 or 350 agents) a jam of dirt-carrying agents frequently occurred around the dump. This was caused by too many agents simultaneously arriving at the dump. However, a

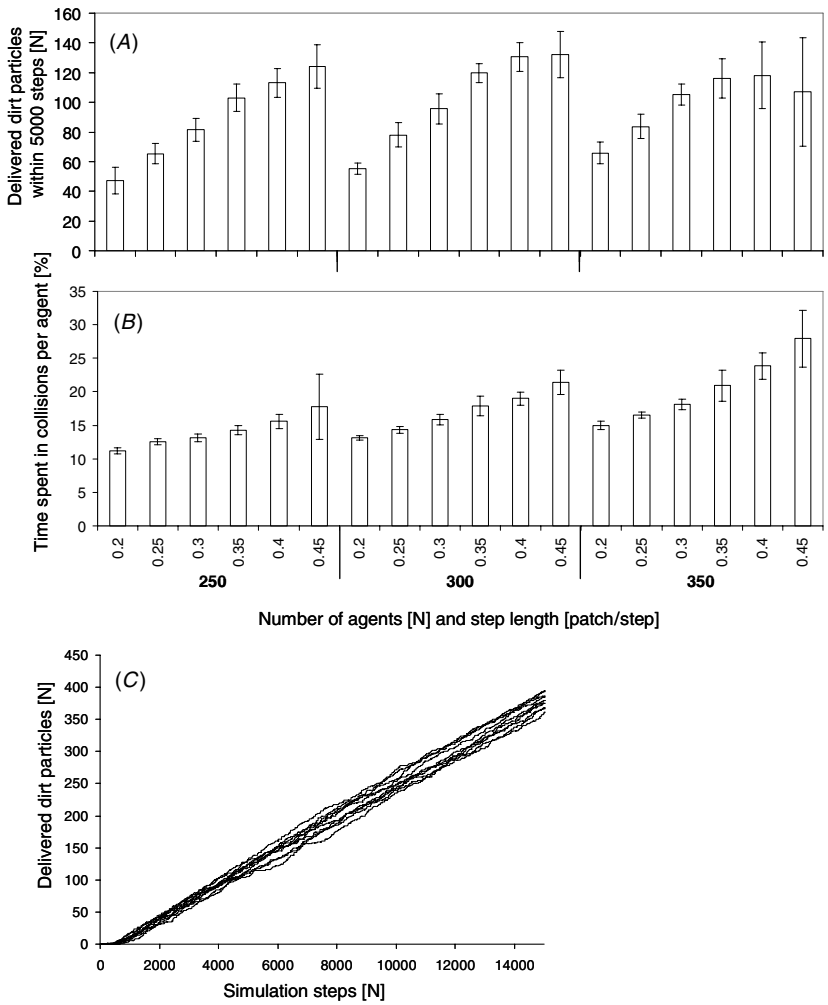

Figure 7. The influence of agent density and locomotion speed on swarm performance and agent interactions. In simulations of the SCS the mean quantity of delivered dirt particles which were counted at the dump within a simulation period of 5000 steps depends on the number of agents in the arena and the locomotion speed of agents (*A*). An increase of swarm performance was accompanied by an increase in the average time (simulations steps) each agent spent in escaping from collisions (*B*). (*C*) shows the temporal evolution of the number of delivered dirt particles collected within 12 long lasting simulation runs performed under optimal conditions. The agent density was 300 and the speed was 0.35 patches per step. The data shown in (*A*) and (*B*) represent the mean ± standard deviation obtained from 12 simulation runs.

balance between dirt-carrying agents arriving at the dump and those leaving the dump is necessary for a sustained delivery of dirt particles. In simulations with 300 agents moving at a step length of 0.35 patches such a balance was already established after 700 simulation steps. Under these conditions, a linear increase of delivered particles was found even in long simulation runs (figure 7(*C*)). Additionally, these model parameters were found to be optimal regarding the collision index (about 7.5) and the path index (about 1.8). This swarm size (300) and locomotion speed (0.35) was found to result in an optimized swarm performance and was therefore used to investigate the robustness of the proposed swarm control strategy.

Using an optimal swarm size and locomotion speed overall swarm performance increased 4.4 times through 's-wave based navigation' in comparison with a scenario in which agents were unable to couple their signal oscillators (27.6 ± 4.7 particles, 12 simulation runs each group).

3.2. Robustness of the swarm control strategy

3.2.1. Robustness of the optimized model: influence of two large obstacles. If two large obstacles were positioned between dirt piles and the dump, dirt-carrying agents were forced to take a longer path (figure 1(*B*)). These obstacles not only blocked the direct walking path between the dirt and dump but also acted as communication obstacles. Such a scenario simulated with 300 agents resulted in a significant reduction of the average quantity of delivered dirt particles compared to the scenario without obstacles across all tested step lengths ($p < 0.05$, paired t-test, $n = 5$, range of step lengths: 0.25–0.45 patches). The best performance was obtained at step lengths of 0.4 and 0.45 yielding 103.8 ± 7.2 and respectively 116.3 ± 6.4 delivered particles after 5000 simulation steps. At these step lengths the collision index was about 10 and the path index was about 3. Both indices were found to be lower compared to smaller step lengths.

3.2.2. Robustness to signal intensity and cycle length fluctuations. A high degree of cycle-to-cycle signal intensity fluctuation may influence the performance of the active collision avoidance behavior and signal oscillator coupling. In the SCS signal intensity fluctuation was modeled by picking the signal intensity from a normal distribution with a mean of 100 (arbitrary units) and a standard deviation of 0.5. Therefore, simulation runs were performed with a much higher signal intensity fluctuation between individual agents (standard deviation of 2.0) and additionally cycle-to-cycle fluctuation of the intrinsic SP was increased (30 ± 2.0). This high variability resulted in a small decrease of swarm performance (SCS: 119.7 ± 6.2 particles, high variability: 96.4 ± 23.0 particles, $p < 0.001$, Mann–Whitney U test, $n = 12$). These simulation results were obtained in a cleaning scenario simulating 300 agents moving at a speed of 0.35 patches per step.

3.2.3. Robustness to agent drop-out. The robustness to agent drop-out was investigated in two steps: (1) within the first 1000 simulation steps 100 randomly chosen agents stopped moving but continued signaling; (2) agents that stopped moving also stopped signaling. The drop-out of 100 agents in the SCS using an optimal agent density and locomotion speed resulted in a significant decrease of the average number of delivered particles from 119.7 ± 6.2 (without drop-out) to 73.3 ± 7.3 (with drop-out) ($p < 0.001$, t-test, 16 simulation runs each group). In scenarios where 100 agents stopped moving and signaling the average number of delivered particles dropped to 63.1 ± 8.6. There was a significant difference between both drop-out scenarios ($p < 0.001$, t-test, 16 simulation runs each group).

3.2.4. Influence of the partial deactivation of PDs. The simulation allowed us to monitor the phase of the disturbance of signal oscillators. It turned out that after the establishment of s-waves, no signal was perceived in about half of the oscillator cycle. Since both sensing (using 4 PDs simultaneously) and signaling are energy demanding, a scenario was developed which allowed us to investigate swarm performance in the SCS after agents switched off their PDs between a signal oscillator phase of 0.15 and 0.7. In such a scenario simulated with 300 agents moving at a speed of 0.35 patches per step a significantly lower number of particles (103.3 ± 10.1) were delivered after 5000 simulation steps ($p < 0.001$, t-test, 12 simulation runs each group). This reduction is small compared to a scenario in which sensing was active throughout the whole oscillator cycle (119.7 ± 6.2 delivered particles).

3.3. Implementation of the swarm control strategy

3.3.1. Competition for dirt-carrying agents. Dirt particles may be regarded as resources and two dumps in the cleaning scenario may compete for dirt-carrying agents. Such a scenario can be easily implemented in the SCS by positioning one dump near the upper left corner and a second dump near of the lower right corner. In such a scenario, both dumps had the same area and distance to the centre. At the end of 12 simulation runs, an average difference of 21.3 dirt particles was found between both competing dumps (sum of both dumps: 33.8 ± 5.8 particles). This significant imbalance ($p < 0.001$) between both dumps even increased to 38.8 particles in scenarios simulated with 350 agents (sum of both dumps: 43.2 ± 6.8 particles).

3.3.2. Asymmetric arrangement of two dumps. In a modified version of the competition scenario, one dump was moved 42 patches closer to the dirt piles. In 17 out of 24 performed simulation runs (simulated with 250 agents), significantly more dirt particles were counted at the closer dump (31.7 dirt particles) than at the competing dump (10.3 dirt particles). From simulation run to simulation run the difference of delivered dirt particles between both dumps was on average 30.8 particles. This imbalance corresponds to 73% of the total number of delivered particles (42 particles). Simulating a higher number of agents (350), only 6 out of 24 runs resulted in a higher number of dirt particles collected at the more closer dump. Nevertheless, the average difference between the number of particles delivered to both dumps was found to correspond to what was found in the competition scenario (76.8%).

3.3.3. Competition between two dumps exhibiting different properties. Competition between two dumps may be influenced by a difference in the intrinsic SP of agents located at the dumps. Such a modification was achieved by reducing the SP of agents on one dump by 9 steps and by 4 steps on the competing dump. These differing oscillator properties resulted in a significantly higher average number of delivered particles at the dump occupied by agents exhibiting a shorter SP (28.1 versus 6.6, $p < 0.001$, t-test, $n = 30$). In a significantly higher proportion of simulation runs that dump occupied by faster signaling agents contained more particles after 5000 simulation steps (26 out of 30 runs, $p < 0.005$, z-test). A similar result was obtained simulating 350 agents. This again resulted in a significantly higher average number of delivered particles at the 'faster' dump (36.3 versus 0.2 particles, $p < 0.001$, t-test, $n = 10$).

3.3.4. Collective decision. Obstacles may be arranged in a way that a longer and a shorter path between a dirt pile and a dump are created (figure 8(*A*)). It was studied whether dirt-carrying agents in such a scenario prefer the shorter (figure 8(*A*), dotted arrow) or the longer path by heading against the direction of s-waves. In this modified cleaning scenario one dump was positioned close to the lower right corner and a single dirt pile was positioned near the upper left corner. This asymmetric arrangement of two gates resulted in a significantly higher number of dirt-carrying agents' ($p < 0.001$, paired t-test, $n = 24$) taking the shorter path (figure 8(*B*) open bars). On average $78.2 \pm 10.0\%$ of dirt-carrying agents took the shorter path. Dividing the shorter path length by the longer path length resulted in an asymmetry index of 0.85.

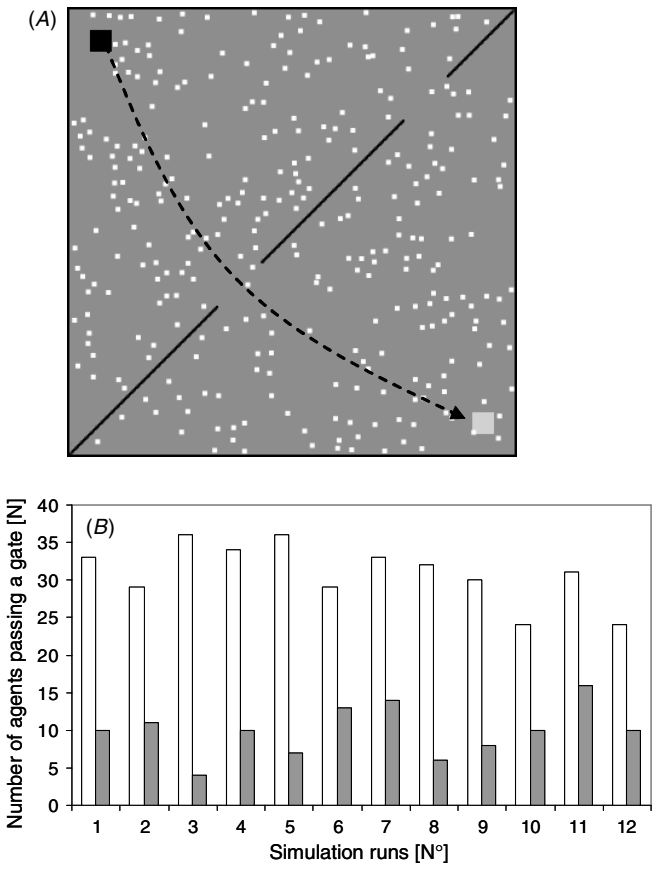

Figure 8. Collective decision making. Diagonally arranged obstacles create two asymmetrically arranged gates. One of these gates created a shorter (dotted arrow) path and the other gate created a longer path between the dirt pile (black square) and the dump (gray square) (*A*). The number of agents passing the gate belonging to the shorter path ((*B*), white bars) and the number of agents passing the gate belonging to the longer path ((*B*), gray bars) were counted in 12 simulation runs.

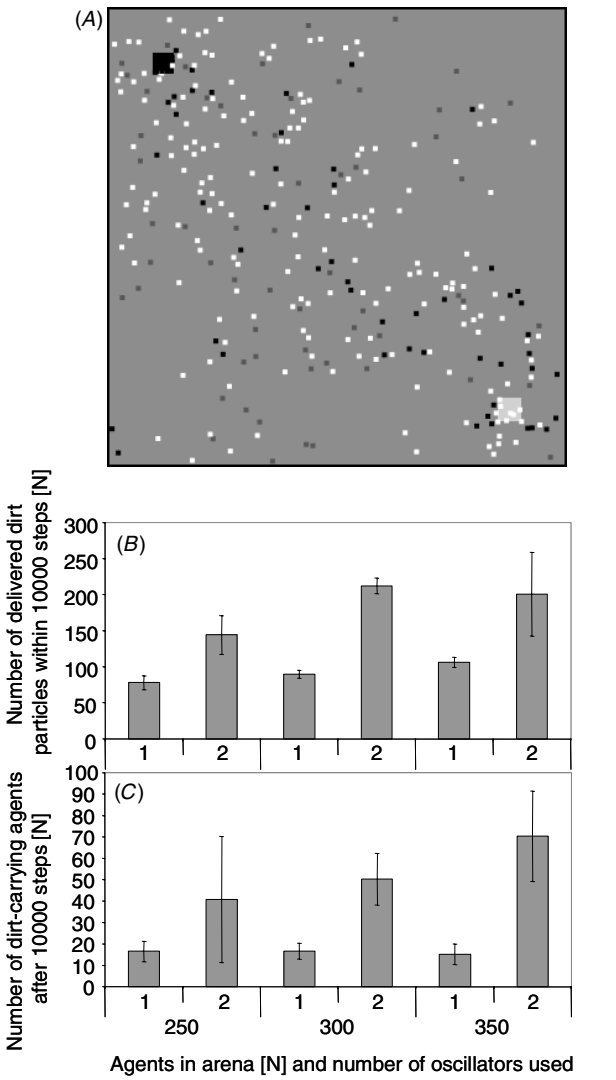

Figure 9. A cleaning scenario based on two oscillators. In a modified version of the cleaning scenario a second oscillator was used to guide agents in search of dirt particles to a dirt pile (black square in (*A*)). A snapshot of such a scenario obtained after 15 000 simulation steps is shown in (*A*). White dots represent agents searching for dirt particles, black dots represent agents carrying dirt particles and gray dots represent relay agents which just perform a pseudo-random walk. Note the self-organized formation of a region of higher agent density along the diagonal axis between the dump (white square) and the dirt pile. The influence of a second oscillator on the number of delivered dirt particles collected at the dump within 10 000 steps is shown in (*B*). The number of dirt-carrying agents found after 10 000 steps is shown in (*C*). Results were obtained from cleaning scenarios differing in the number of simulated agents (step length 0.35 patches). Bars represent the mean number of delivered dirt particles obtained from 10 simulation runs ± standard deviation.

3.3.5. Two-oscillator scenario. For the investigation of the influence of a second signal oscillator, only one dirt pile was positioned close to the upper left corner and one dump was positioned close to the lower right corner (figure 9(*A*)). On average a significantly higher number of dirt particles were delivered after 10 000 simulation steps in scenarios simulated with 250, 300 or 350 agents compared to the same scenario with only one oscillator and the same amount of agents (0% relays) ($p < 0.001$, Mann–Whitney U test, 10 simulation runs for each group) (figure 9(*B*)). Furthermore, a significantly higher number of dirt-carrying agents ($p < 0.001$, Mann–Whitney U test, $n = 10$) was found after 10 000 simulation steps (figure 9(*C*)). Agents in these scenarios were moving at a step length of 0.4 patches. Simulations revealed that in scenarios with 350 agents the dirt cluster was quickly surrounded by 'searching agents'. This sometimes resulted in weak swarm performance and accounted for the higher standard deviation, as shown in figure 9(*B*). In scenarios with one oscillator, a balance between dirt-carrying agents delivering their particles and those picking up particles was established after about 1200 steps. In contrast, in scenarios with two oscillators, this balance was achieved much later, after about 7000 steps. In a control scenario in which two oscillators were simulated but oscillator coupling was disabled only 37.1 ± 6.5 dirt particles were collected at the dump after 10 000 simulation steps (10 simulation runs). Therefore, the oscillator-based swarm strategy improved swarm performance 5.7 times within this simulation period.

4. Discussion

The miniaturization of microrobots is accompanied by limitations of communication capabilities and agility. In order to guarantee the completion of a complex swarm task, swarm intelligence is able to compensate for the simplicity of individual swarm members [6]. The cleaning scenario investigated in the current study was chosen because swarm intelligence is needed for a rapid transfer of dirt particles to the dump and because of its applicability to real-world scenarios such as garbage collection in hazardous areas. The current study proposes a swarm control strategy which enables members of a swarm of simple agents to accomplish a find and retrieve task without path planning, self positioning, external navigation cues, goal communication and/or a connection to a central master. Navigation in a complex cleaning scenario was achieved by signaling waves, which were established in a self-organized manner by the coupling of signal oscillators.

There are few descriptions of how mathematical models of an array of two-dimensional coupled oscillators behave. Ermentrout described such an array of excitatory-inhibitory coupled neuronal oscillators that resulted in either concentric waves or spiral waves [7]. The observed pattern of activity depends on both the type and the strength of coupling. As soon as oscillators are moving, coupling strength will constantly change over time and a mathematical description becomes very difficult. Therefore, in our study, the simultaneous interaction of many hundreds of agents was simulated in discrete time steps in which each agent increments its oscillator cycle and obeys simple behavioral rules.

Mexican waves [8], known from soccer stadiums, are very similar to s-waves, since in both cases waves are generated by the synchronous activity of densely packed individuals exhibiting a limited sensor range. However, there are some major differences: individuals taking part in the spreading of waves may not be regarded as oscillators and a frequently found cyclic activity arises from the circular design of stadiums, which favors circling waves. Furthermore, a critical mass of simultaneously active fans are necessary for the initiation of Mexican waves. In the oscillator-based communication strategy waves are generated at a rate corresponding to the free-run period of those oscillators initiating s-waves and only one agent with a shorter SP is sufficient in order to initiate concentric s-waves.

In simulations in which agents were assigned to only one signal oscillator agents need to be rather homogeneously spaced in order to maintain a propagation of s-waves throughout the arena. The active collision avoidance strategy investigated in the cleaning scenario improved such spacing and hence swarm performance due to the following reasons: (1) the chance of an accidental encounter of a dirt pile or a dump was increased; (2) searching agents make way for dirt-carrying agents. This result suggests such a simple type of collision avoidance for swarm robots lacking an elaborate active collision avoidance, which is usually realized by additional hardware.

In the absence of an elaborate active collision avoidance and limited sensor range, collisions are inevitable. The implementation of an active escape strategy performed after collisions decreased swarm performance significantly. It turned out that such a strategy delays the delivery of dirt particles in the SCS by keeping searching agents from performing a pseudo-random walk and dirt-carrying agents from moving against the wave-front. In contrast, the suggested passive escape strategy resulted in a better swarm performance and may be the only way to free agents after collisions in a swarm of primitive microrobots lacking an elaborate sensor system avoiding collisions.

In the current simulation self-organization can be found in several stages of the cleaning scenario: (1) in the establishment of s-waves propagating from agent to agent; (2) in the strengthening of the signaling chain by the presence of dirt-carrying agents between the dirt cluster and the dump (see figure 9(*A*); (3) by maintaining the triggering of s-waves at the dump after dirt-carrying agents delivered dirt particles. Therefore, the suggested swarm control strategy extensively makes use of self-organization emerging from the interaction of agents obeying simple behavior rules.

The main task of the cleaning scenario is the transport of particles, which forms the basis for other swarm scenarios such as foraging [9, 24]. However, the currently proposed swarm control strategy is different from foraging behavior, which is known from real robot swarms, with respect to target competition. The introduction of a second dump in the current study resulted in an imbalance of delivered particles between both dumps (sharing the same properties). The reason for this imbalance arises from the fact that once an s-wave was initiated at one dump the competing dump will trigger s-waves shortly before an s-wave of the other dump already approaches. The randomized start of individual oscillator cycles and the random distribution of agents at the beginning of each simulation prevented a reliable prediction of which dump first initiates s-waves. This holds true even in a scenario in which one dump is located closer to both dirt piles.

The amount of collected dirt particles at both dumps could, however, be properly controlled by changing the free-run cycle of agents at both dumps differently. This property of the oscillator-based swarm control could be implemented in robot scenarios in which robots are able to recognize the quality of a target. This would allow individual agents to attract more dirt-carrying agents to a dump of better quality (e.g. closer to a dirt pile or larger). In cleaning scenarios in which two signal oscillators were implemented in each agent, this property of swarm control can be used to attract more agents to a dirt pile of better quality and transfer particles to a more attractive dump. These self-emergent swarm dynamics are inherent properties of the suggested swarm control strategy and would allow an optimized exploitation of resources of different qualities. This has been shown for the foraging behavior of honey-bee colonies [32].

Within a few oscillator cycles the oscillator-based control strategy automatically switches to a new target as soon as the quality of a target becomes worse (data not shown). This emphasizes an important difference between the oscillator-based control strategy and a signal wave propagation, which is maintained by a cascaded release of chemical compounds after

the perception of a supra-threshold chemical signal. This kind of wave generation can be found in slime mold aggregations in which agents move against a chemical gradient before they go into a refractory state, which prevents an instantaneous backward locomotion [4, 27].

Higher agent densities not only increase transport capacity but also increase the time spent in escaping from collisions, which, on the other hand, counteracts swarm performance. This result corroborates findings in real robot scenarios in which the interaction among a small group of robots was shown to delay the time to accomplish a task [2, 19, 21, 35]. In the current study, agent interactions not only increased with swarm size but also increased linearly with locomotion speed (figure 7(*B*)). Therefore, an optimal agent density moving at an optimal speed could be determined for the SCS (300 agents, step length of 0.35 patches). At this speed the collision index and the path index was found to be lowest, which indicates an optimal locomotion speed in relation to the speed of signal oscillators (30 steps).

Obstacles disturbed the concentric spreading of s-waves heavily. However, in successive oscillator cycles the front of s-waves circumvented obstacles as did the dirt-carrying agents. Due to a more asynchronous arrival of dirt-carrying agents at the dump, swarm performance increased linearly with locomotion speed in scenarios with two large obstacles. Obstacles which forced agents to choose between two paths of different lengths revealed another property of the oscillator-based swarm control: concentric s-waves passed a closer gate earlier compared to a more distant gate (figure 8(*A*), lower gate). Therefore, agents heading against the 'leader signal' automatically preferred the shorter path. A similar result was obtained in a simulation of a cleaning scenario based on a different control strategy, which was derived from the trophallaxis behavior of real bees [31]. Bees transfer a certain amount of crop to other bees in a swarm and thereby create a gradient of the distributed crop in a swarm. In a simulated cleaning scenario this gradient was used to guide dirt-carrying agents to the dump. The trophallaxis-derived strategy resulted in an even higher percentage of agents (about 82%) preferring the shorter of two paths exhibiting an asymmetry index of 0.85. The reason for this difference may be found in the differing complexity of agents. Agents in the trophallaxis-derived simulation are equipped with an elaborate collision avoidance system, 6 PDs and 6 LEDs and high agility.

The robustness to agent drop-out and signal fluctuation as well as oscillator cycle fluctuations was remarkable and emphasizes the fault tolerance of the distributed oscillator-based swarm control. In scenarios with only one oscillator the PDs of agents could be switched off for about half of the oscillator cycle without affecting swarm performance much. This is important with respect to the tradeoff in miniaturization and the energetic demands of the 4 PDs implemented in the I-Swarm robot. However, as soon as two signal oscillators are realized in a cleaning scenario this energy saving method fails because the signaling of both oscillators is independent and requires permanent sensing.

A communication system which relies on faint flashes of light is less energy demanding compared to the transmission of a complex binary code. Furthermore, the calculation of the disturbed cycle length of signal oscillators requires only little computational effort. Due to these reasons and due the simplicity of the reaction-based agent behavior the oscillator-based swarm control seems to be promising for a proper control of a swarm of simple microrobots engaged in different kinds of search and retrieve tasks.

5. Conclusions and future work

Instead of implementing a complex communication system in a swarm of primitive microrobots which undeniably suffers from a high degree of signal interference, the current study demonstrates how self-organized synchronization of primitive signal oscillators provide the basis for a proper control of agents in a cleaning scenario. In such a scenario this swarm control strategy resulted in a manifold increase of swarm performance which arises form the navigation cue provided by waves of synchronized signaling. Swarm performance was further improved by the implementation of a second signal oscillator which guides agents in search of dirt particles to a dirt cluster.

The suggested control strategy is highly adaptive to changes in the environment and robust to agent drop-out as well as signal intensity fluctuations and fluctuations of the oscillator cycle length. S-waves were successful in guiding agents to a target and additionally provide the basis of a simple form of active collision avoidance. Finally, it was shown that agents heading against the front of s-waves prefer the shorter of two alternative paths and obstacles were successfully circumvented. For all investigated cleaning scenarios there exists an optimal swarm size and locomotion speed which yields the best swarm performance.

As soon as I-Swarm microrobots are available, the oscillator-based swarm control strategy and the suggested behavior rules will be investigated in a real robot swarm engaged in a cleaning scenario. In the future, microrobots will have improved capabilities which allow them to carry small particles, act in complex environments and become independent from a constant power supply. These are the requirements for realistic missions of microrobots in hazardous or hardly accessible areas (e.g. pipes). A distributed swarm control, as is suggested in the current study, will then enable members of a swarm to navigate in a constantly changing environment.

Acknowledgments

This work is supported by the EU IST-FET-open project (IP) 'ISwarm', no 507006.

References

[1] Balch T and Arkin A C 1994 Communication in reactive multiagent robotic systems *Auton. Robots* **1** 27–52
[2] Beckers R, Holland O E and Deneubourg J L 2000 *Prerational Intelligence: Adaptive Behavior and Intelligent*

Systems Without Symbols and Logic (Dordrecht: Kluwer) 549–63
[3] Bellman R E 1957 *Dynamic Programming* (New York: Princeton university Press)
[4] Camazine S, Deneubourg J L, Franks N R, Sneyd J, Theraulaz G and Bonabeau E 2003 *Self-Organization in Biological Systems* (Princeton, NJ: Princeton University Press)
[5] Clark M R and Anderson G T 2000 Coupled oscillator control of autonomous mobile robots *Auton. Robots* **9** 189–98
[6] Deneubourg J L and Gross S 1989 Collective patterns and decision making *Ethol. Ecol. Evol.* **1** 295–311
[7] Ermentrout B 2005 Neural oscillators *Lecture Notes in Mathematics* (Berlin: Springer) 69–106
[8] Farkas I, Helbing D and Vicsek T 2002 Mexican waves in an excitable medium *Nature* **419** 131–2
[9] Goldberg D and Mataric M J 2000 Robust behavior-based control for distributed multi-robot collection tasks *IEEE Trans. Robot. Autom.*
[10] Goss J L, Deneubourg J L and Franks N 1991 The dynamics of collective sorting: robot-like ants and ant-like robots *Proc. 1st Int. Conf. on Simulation of Adaptive Behavior on From Animals to Animats (Paris)* pp 356–63
[11] Habib M K, Asama M J, Endo I, Matsumoto A and Ishida Y 1992 Simulation environment for an autonomous decentralized multi-agent robotic system *IEEE/RSJ Int. Conf. on Int. Rob. and Syst.* pp 1550–7
[12] Hartbauer M, Kratzer S, Steiner K and Römer H 2005 Mechanism for synchrony and alternation in song interactions of the bushcricket *Mecopoda elongata* (Tettigoniidae: Orthoptera) *J. Comp. Physiol.* A **191** 175–188
[13] Hartbauer M and Roemer H 2006 Decentralised microrobot swarm communication via coupled oscillators *Proc. 1st IEEE/RAS-EMBS Int. Conf. on Biomedical Robotics and Biomechatronics (Pisa, Italy)*
[14] Hsin Sit T C, Liu Z, Ang M H and Guan Seah W K 2007 Multi-robot mobility enhanced hop-count based localization in ad hoc networks *Robot. Auton. Syst.* **55** 244–52
[15] Holland O E, Melhuish C and Hoddell S 1997 Chorusing and controlled clustering for minimal mobile agents *4th European Conf. on Artificial Life (Brighton, UK)*
[16] Ichikawa S and Hara F 1994 An experimental realization of cooperative behavior of multi-robot system *Distrib. Auton. Robot. Syst.* 224–34
[17] Ishiguro A and Shimizu M 2004 Don't try to control everything!: an emergent morphology control of a modular robot *Proc. IEEE/RS Int. Conf. on Intelligent Robots and Systems (Sendai, Japan)*
[18] Jadbabaie A, Motee N and Barahona M 2004 On the stability of the Kuramoto model of coupled nonlinear oscillators *Proc. American Control Conf. (Boston, MA)*
[19] Krieger M J, Billeter J B and Keller L 2000 Ant-like task allocation and recruitment in cooperative robots *Nature* **406** 992–5
[20] Kurabayashi D, Okita K and Funato T 2006 Obstacle avoidance of a mobile robot group using a nonlinear oscillator network *Proc. IEEE/RSJ Int. Conf. on Intelligent Robots and Systems (Beijing, China)*
[21] Lerman K, Martinoli A and Ijspeert A 2001 A macroscopic analytical model of collaboration in distributed robotic systems *Artif. Life* **7** 375–93
[22] Mataric M J, Sukhatme G S and Ostergaard E H 2003 Multi-robot task allocation in uncertain environments *Auton. Robots* **14** 255–63
[23] Nicolescu M N and Mataric M J 2002 A hierarchical architecture for behavior-based robots *1st Int. Joint Conf. on Autonomous Agents and Multi-Agent Systems (Bologna, Italy)*
[24] Nitz E, Arkin R C and Balch T 1993 Communication of behavioral state in multi-agent retrieval tasks *Proc. 1993 IEEE Int. Conf. on Robotics and Automation (Atlanta, GA)* p 588–94
[25] O'Hara K J and Balch T R 2004 Distributed path planning for robots in dynamic environments using a pervasive embedded network *Proc. 3rd Int. Joint Conf. on Autonomous Agents and Multiagent Systems (New York)* vol 3 pp 1538–9
[26] Parker L E 1996 On the design of behaviour-based multi-robot teams *Adv. Robot.* **10** 547–78
[27] Resnick M 1994 *Turtles, Termites and Trac Jams: explorations in Massively Parallel Microworlds* (Cambridge, MA: MIT Press)
[28] Rodin E Y and Amin S M 1998 Intelligent navigation for an autonomous mobile robot *Proc. Int. Symp. on Int. Control (Arlington)* pp 366–9
[29] Fertschai I, Stradner J and Römer H 2007 Neuroethology of female preference in the synchronously singing bushcricket *Mecopoda elongata* (Tettigoniidae; Orthoptera): why do followers call at all? *J. Exp. Biol.* **210** 465–76
[30] Rybski P E, Larson A, Schoolcraft A, Osentoski S and Gini M 2002 Evaluation of control strategies for multi-robot search and retrieval *7th Int. Conf. on Intelligent Autonomous Systems (Marina del Rey, CA)* pp 281–8
[31] Schmickl T and Crailsheim K 2006 Trophallaxis among swarm-robots: a biologically inspired strategy for swarm robotics *Proc. 1st IEEE/RAS-EMBS Int. Conf. on Biomedical Robotics and Biomechatronics (Pisa, Italy)*
[32] Seeley T D and Buhrman S C 2001 Nest-site selection in honey bees: how well do swarms implement the 'best-of-N' decision rule? *Behav. Ecol. Sociobiol.* **49** 416–27
[33] Sismondo E 1990 Synchronous, alternating, and phase-locked stridulation by a tropical katydid *Science* **249** 55–8
[34] Steels L 1990 Cooperation between distributed agents through self-organisation *Proc. Intelligent Robots and System*
[35] Sugawara K and Sano M 1997 Cooperative acceleration of task performance: foraging behavior of interacting multi-robots system *Physica* D **100** 343–54
[36] Tkahashi N, Yokoi H and Kakazu Y 2000 Coupled oscillator system for amoeba-like robot control *Intell. Auton. Syst.* **6** 99–104
[37] Wang T and Zhang H 2003 Multi-robot collective sorting with local sensing *Proc. IEEE Intelligent Automation Conf. IAC (Hong Kong, China)*
[38] Zhong Y, Liang J, Guochang G, Zhang R and Yang H 2002 An implementation of evolutionary computation for path planning of cooperative mobile robots *Proc. Intelligent Control and Automation (Shanghai, China)*